Dependence of Wave Speed on Acidity and Initial Bromate Concentration in the Belousov-Zhabotinsky Reaction-Diffusion System

Matthew D. Eager, Marianne Santos, Milos Dolnik, Anatol M. Zhabotinsky, Kenneth Kustin, and Irving R. Epstein

J. Phys. Chem., **1994**, 98 (42), 10750-10755• DOI: 10.1021/j100093a013 • Publication Date (Web): 01 May 2002

Dependence of Wave Speed on Acidity and Initial Bromate Concentration in the Belousov−Zhabotinsky Reaction−Diffusion System

Matthew D. Eager, Marianne Santos, Milos Dolnik, Anatol M. Zhabotinsky,* Kenneth Kustin,* and Irving R. Epstein

Department of Chemistry, Brandeis University, Waltham, Massachusetts 02254-9110

Received: January 21, 1994; In Final Form: July 21, 1994[⊗]

Propagation of chemical waves in the Belousov−Zhabotinsky (BZ) reaction−diffusion system is simulated with an improved Oregonator-type model in the entire region of propagation of solitary waves. The dependence of wave speed on bromate concentration and acidity is determined. Deviations from linear dependence of the speed on the quantity $\theta^{0.5} = (h_0([HBrO_3] + [BrO_3^-]))^{0.5}$ (h_0 = Hammett acidity function) are found at both high and low θ. The model predicts that the wave speed has a maximum at high values of θ. Comparison of experimental data with simulations shows that saturation of the reactive layer by oxygen can significantly increase the region in parameter space that supports propagation of solitary waves.

Introduction

Several types of waves, primarily front, pulse (solitary wave), and wave train, are known to propagate in reaction−diffusion systems. The Belousov−Zhabotinsky (BZ) reaction−diffusion system is the only homogeneous chemical system where the dependence of the pulse (not the front) speed on initial reagent concentrations has been studied experimentally.[1−6] For such a complex system, the strikingly simple dependence of pulse speed on initial reagent concentrations has led to an analysis based solely on propagation of the leading front of the pulse. This theoretical approach is restrictive, because the pulse speed should depend on several factors, in particular, on excitation threshold, pulse amplitude, and pulse width.

For example, in their pioneering work Field and Noyes[1] found that the wave speed (v) in the ferroin-catalyzed BZ reaction−diffusion system is linearly dependent on the square root of the proton and bromate ion concentration product $(([H^+]\cdot[NaBrO_3])^{0.5} \equiv \Theta^{0.5})$, with only minor dependence on the other reagent concentrations. The authors' attribution of this result to the dependence of the speed of the reaction front on the rate of the autocatalytic oxidation of metal ion catalyst by bromous acid corresponds to the original Fisher and Kolmogorov−Petrovsky−Piskunov (KPP)[7] theory of propagation of an autocatalytic reaction without a threshold.[8−10] However, the KPP theory predicts a direct proportionality of v on $\Theta^{0.5}$. In subsequent publications, propagation of the solitary oxidation wave (SOW) in the BZ reaction−diffusion system was also analyzed as propagation of its leading front. The fitting of v by a linear form, such as $v = -b + a\Theta^{0.5}$, has been widely accepted,[3−6] with the notion that the deviation from the direct proportionality is due to the influence of the elevated concentration of Br^- in front of the propagating wave.[11]

More general treatments of wave propagation have shown, however, that pulse speed depends on the ratio of the amplitude of the front to the excitation threshold, and on the pulse width,[8−10] which in the BZ reaction also depends on the acidity and the total bromate concentration ($[BrO_3^-]_T$). In fact, Nagy-Ungvarai *et al.*[6] have shown that with cerium as catalyst the linear dependence on $\Theta^{0.5}$ is valid in only part of the concentration space. This observation raises the question whether the deviation from linear dependence is due to a deviation of the autocatalysis rate from the known simple dependence, or whether the pulse amplitude and pulse width start to play a role.

In this paper, we present a numerical study of SOW propagation in the BZ reaction−diffusion system to elucidate the problem and find out whether it is possible to separate the effect of the autocatalysis rate from other factors determining the SOW speed dependence on concentration. Analysis of how pulse speed and autocatalysis rate depend on concentration is carried out for the first time in the full range of concentrations where stationary pulse propagation can occur. Results of computer simulations are compared with previous and new experimental data for SOWs propagating in systems with a reduced catalyst steady state.

Experimental Section

Materials. $Ce(SO_4)_2\cdot 4H_2O$, $NaBrO_3$ (Janssen), $CH_2(COOH)_2$ (Aldrich), KBr (Fisher), and H_2SO_4 (Mallinckrodt) were of reagent grade. Mixtures of bromomalonic (BrMA), dibromomalonic, and malonic acids were prepared by direct bromination of malonic acid according to the net reaction:

$$BrO_3^- + 2Br^- + 3H^+ + 3CH_2(COOH)_2 \rightarrow 3BrCH(COOH)_2 + 3H_2O$$

The concentration of BrMA in the stock solution was estimated according to data from Försterling et al.[12]

Methods. A 1.2 mm thick layer of solution was placed either in a standard plastic Petri dish or between a pair of glass plates. The temperature was 23 ± 0.5 °C.

Waves were initiated with a 0.3 mm Ag wire that had been stored in 10 M H_2SO_4 and wiped dry immediately before being placed in contact with the working solution.

Wave propagation was monitored via transmitted light from a deuterium arc lamp with a video camera equipped with a Corning UV filter (maximum transmittance at about 360 nm).

Model

Our simplified reaction scheme for the bromate−catalyst−BrMA system is as follows:

$$H^+ + Br^- + HOBr \rightleftarrows Br_2 + H_2O \qquad (R1)$$

[⊗] Abstract published in *Advance ACS Abstracts,* October 1, 1994.

0022-3654/94/2098-10750$04.50/0

$$H^+ + Br^- + HBrO_2 \rightleftarrows 2HOBr \quad (R2)$$

$$H^+ + Br^- + HBrO_3 \rightleftarrows HBrO_2 + HOBr \quad (R3)$$

$$2HBrO_2 \rightleftarrows HOBr + HBrO_3 \quad (R4a)$$

$$H^+ + HBrO_2 \rightleftarrows H_2BrO_2^+ \quad (R4b)$$

$$HBrO_2 + H_2BrO_2^+ \rightleftarrows HOBr + HBrO_3 + H^+ \quad (R4c)$$

$$H^+ + BrO_3^- \rightleftarrows HBrO_3 \quad (R5a)$$

$$H^+ + HBrO_3 + HBrO_2 \rightleftarrows HBrO_2^+ + BrO_2^\bullet + H_2O \quad (R5b)$$

$$BrO_2^\bullet + H^+ \rightleftarrows HBrO_2^+ \quad (R5c)$$

$$Red + HBrO_2^+ \rightleftarrows Ox + HBrO_2 \quad (R6)$$

$$Ox + B \rightleftarrows Red + B^\bullet + H^+ \quad (R7)$$

$$B^\bullet \rightarrow qBr^- \quad (R8)$$

$$B \rightarrow Br^- \quad (R9)$$

Here "Red" is the reduced form of the catalyst: Ce^{3+}, or Fe(phen)$_3^{2+}$; "Ox" is the oxidized form: Ce^{4+}, or Fe(phen)$_3^{3+}$; B = $CH_2(COOH)_2$ + $CHBr(COOH)_2$.

We use here the simplified version of the model derived in ref 13. With an additional quasisteady state approximation for [$HBrO_2^+$], the model takes the form

$$\frac{dX}{dt} = \frac{-k_2X + k_3A}{k_2X + k_3A}\left(qk_7k_8\frac{BZ}{k_8 + k_{-7}h_0(C-Z)} + k_9B\right) - 2k_4X^2 + k_5h_0AX - k_{-5}U^2$$

$$\frac{dZ}{dt} = k_6U(C-Z) - k_{-6}XZ - \frac{k_7k_8BZ}{k_8 + k_{-7}h_0(C-Z)}$$

$$U = \frac{-k_6(C-Z) + [(k_6(C-Z))^2 + 8k_{-5}(2k_5h_0AX + k_{-6}XZ)]^{1/2}}{4k_{-5}} \quad (1)$$

Here X = [$HBrO_2$], Z = [Ox], U = [$HBrO_2^+$], A = [$HBrO_3$] = $h_0A_0/(h_0 + K_{5a})$, A_0 = [$NaBrO_3$]$_0$, $K_{5a} = k_{-5a}/k_{5a}$, B = [$CH_2(COOH)_2$] + [$CHBr(COOH)_2$], $C = Z$ + [Red], h_0 = Hammett acidity function,[14] $k_4 = k_{4a}(1 + 0.87h_0)$, $k_5 = k_{5b}$, $k_{-5} = (k_{-5b}k_{-5c})/(k_{5c}h_0)$. We further define $h_0A_0 = \theta$.

The rate constants used in the simulations are summarized in Table 1. In all simulations B = 0.12 M. The parameters A_0, h_0, q, and C are varied. To simulate wave propagation, we add diffusion terms to the differential equations of model 1, with $D_x = 1.5 \times 10^{-5}$ cm^2 s^{-1} and $D_z = 2 \times 10^{-6}$ cm^2 s^{-1}.

According to the KPP theory[7] the speed of the wave front is proportional to $\Psi^{0.5}$, where $\Psi = \partial V/\partial C$ is the derivative of the rate (V) of production of the autocatalytic species with respect to the concentration (C) of that species. The derivative is to be taken at the initial unstable steady state. Since we are interested in a stable but excitable steady state rather than an unstable steady state, it is not possible to apply directly the simple KPP theory to eq 1, where $V = dX/dt$. However, it seems reasonable that the KPP theory may be employed as a first approximation in some range of parameters. First, we make a singular perturbation approximation[15] and replace the wave propagation by propagation of the wave front with $Z = Z_{ss}$, where Z_{ss} is the steady-state concentration of Z. As a result of this approximation, we obtain a bistable system with three steady states: an initial, stable steady state (X_1), which coincides with the steady state of the full system (X_{ss},Z_{ss}); an intermediate, unstable steady state (X_2), which corresponds to the excitation threshold; and a stable steady state (X_3), which corresponds to the maximum of X, i.e., to the wave amplitude. The profile and speed of the front in this system will be close to that given by the KPP theory if the threshold of excitation ($X_2 - X_1$) is relatively small with respect to the amplitude of the front ($X_3 - X_1$). In this case, we expect the speed (v) to be proportional to $\Psi^{0.5}$ if the derivative is taken at X_2. This approximation puts in mathematical terms the most widely accepted point of view about the wave speed dependence on initial reagent concentrations in the BZ reaction–diffusion system.

To separate the effects of the threshold and amplitude on the wave speed from that of $\Psi^{0.5}$, we calculated v and $\Psi^{0.5}$ in parallel.

TABLE 1: Rate Constants for Eqs R2–R9[a]

	cerium		ferroin
k_2 (M^{-2} s^{-1})		2×10^6	
k_{-2} (M^{-1} s^{-1})		0	
k_3 (M^{-2} s^{-1})		2.0	
k_{-3} (M^{-1} s^{-1})		0	
k_4 (M^{-1} s^{-1})		3×10^3	
k_{-4} (M^{-1} s^{-1})		0	
k_5 (M^{-2} s^{-1})		33	
k_{-5} (M^{-1} s^{-1})		4.2×10^6	
k_6 (M^{-1} s^{-1})	6.2×10^4		1×10^8
k_{-6} (M^{-1} s^{-1})	2×10^4		3.0
k_7 (M^{-1} s^{-1})	0.4		–
k_{-7} (M^{-1} s^{-1})	0		–
k_8/k_{-7} (M^2)	–		1×10^{-5}
k_7k_8/k_{-7} (M s^{-1})	–		1×10^{-5}
k_9 (s^{-1})	3.3×10^{-6}		6×10^{-6}
k_{5a} (M)		0.2	

[a] Rate constants k_2–k_{-5} are catalyst independent.

Methods of Computation

For numerical analysis of the space-independent (point) model which corresponds to the well-stirred system, we employed the CONT numerical bifurcation and continuation package.[16] The rate derivative Ψ was determined in the excitation cycle of the point system. The cycle of excitation was started from the following initial conditions: $X_0 = X_{ss} + \delta$, $Z_0 = Z_{ss}$, where X_{ss} and Z_{ss} are the steady-state values and $\delta = 2 \times 10^{-6}$ M. The derivative of the rate of X production was calculated as the derivative of the right-hand side of the first equation in the model (1) with respect to X. The maximum of the derivative was always found in the close vicinity of the initial point. This maximum value was chosen as the characteristic derivative Ψ.

Simulations of the wave propagation in one dimension were performed using a finite-difference approximation to the differential equations of model 1. The corresponding system of ordinary differential equations was then solved with the LSODE subroutine,[17] using an analytic Jacobian matrix. The numerical stability of the algorithm was improved as described in ref 18. Typical error tolerances were 1×10^{-8} relative and 1×10^{-12} absolute. Simulations were performed on an IBM RISC 6000 workstation Model 340. We used 400 gridpoints for the 10 mm physical length. Neumann (zero flux) boundary conditions were employed. As initial conditions, the variables were assigned their steady-state values for 99% of the length; along the remaining 1% of the length the value of X was increased to 1×10^{-5} M. This perturbation was enough to start wave propagation. A stationary wave profile soon became established

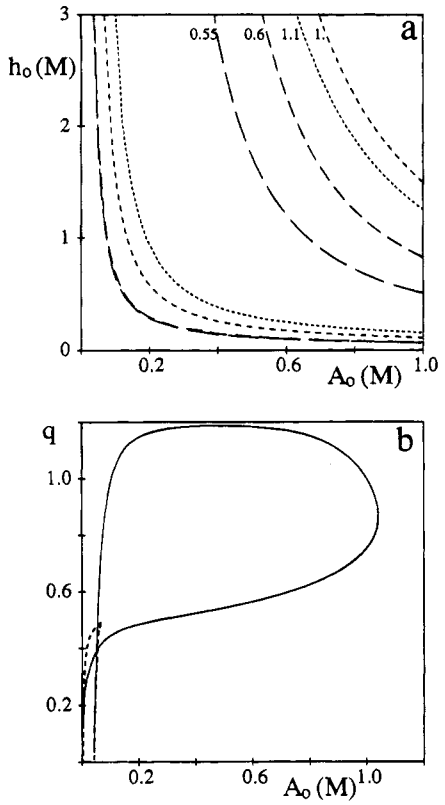

Figure 1. Bifurcation diagrams of eqs 1 for the cerium-catalyzed system, $C = 6 \times 10^{-3}$ M, $B = 0.12$ M. (a) Lines of supercritical Hopf bifurcation in the (h_0,A_0)-plane; q values are shown in the figure. (b) Bifurcation diagram in the (q,A_0)-plane: solid line, Hopf; dashed line, saddle-node bifurcation; $h_0 = 1.5$ M.

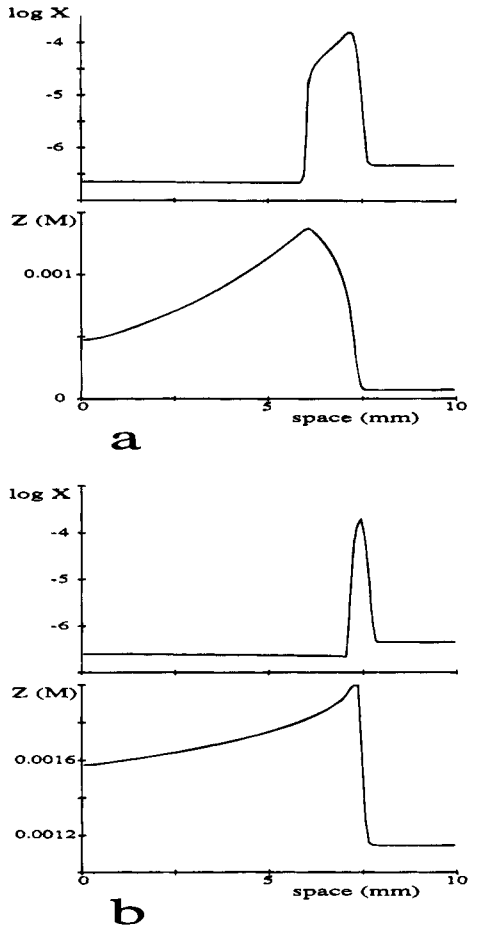

Figure 2. Simulated profile of a stationary propagating pulse for the cerium- (a) and the ferroin-catalyzed (b) BZ reaction–diffusion system. Initial reagent concentrations (in M): $h_0 = 0.5$, $A_0 = 0.3$, $B = 0.12$, $C = 6 \times 10^{-3}$ (a), $C = 2 \times 10^{-3}$ (b). Waves propagate from the left to the right.

in the first 10% of the system length. The wave speed was determined from the trajectory of the maximum of the X profile.

Simulation Results

Determination of the Region of Solitary Wave Propagation. Figure 1a shows the lines of supercritical Hopf bifurcation of the point system in the (h_0,A_0)-plane at various values of the stoichiometric factor q. As q increases, the lower Hopf line moves up. The upper Hopf line moves up when q increases from 0.45 to 0.85, and then begins to move down, until at q slightly less than 1.2 the oscillatory region disappears. The bifurcation diagram in Figure 1b shows that in the (q,A_0)-plane the Hopf line forms a closed loop with a maximum at $q = 1.188$.

The oscillatory region lies inside the region confined by the Hopf lines (Figure 1b), and bands of excitability are located around the oscillatory region. The regions of single wave propagation lie inside the excitability bands. We assume that one boundary of the SOW region coincides with the Hopf line. The second boundary was found by direct simulation of the wave propagation (see Experimental Results). Figure 2 shows the simulated shape of the pulse in both cerium- and ferroin-catalyzed systems.

Dependence of Wave Speed v and Rate Derivative Ψ on θ. Figure 3a shows the dependence of the wave speed v on $\theta^{0.5}$ in a cerium-catalyzed system with $q = 1.2$ for three different values of A_0. When A_0 is relatively small ($A_0 = 0.3$ M) the wave speed is linear in $\theta^{0.5}$ over almost the entire physically reasonable range of h_0. For higher A_0 the dependence deviates from a straight line at higher values of θ. There is also a deviation from linear dependence at low values of θ close to the boundary of wave propagation (see insets in Figures 3a and 4a).

Figure 4a shows similar plots at constant h_0. The wave speed in this case strongly deviates from a linear dependence for all the curves. At a given value of $\theta^{0.5}$ the speed is higher for higher values of h_0 and for lower values of A_0. Clearly the wave speed is not a function only of θ.

Figure 5a shows the wave speed dependence for a ferroin-catalyzed BZ reaction with $q = 1.2$ in the range of θ corresponding to the experimental measurements of Field and Noyes.[1] In this range the wave speed is a linear function of $\theta^{0.5}$ both for constant A_0 and for constant h_0. When the range of θ is extended, a significant deviation from linearity appears (Figure 5b).

A maximum in v at high values of θ was found in both the ferroin- and the cerium-catalyzed systems.

The dependence of $\Psi^{0.5}$ on $\theta^{0.5}$ is shown in Figures 3b and 4b for a cerium-catalyzed BZ reaction. In the cerium case the curves are linear at intermediate values, but they deviate from linearity at both ends of the θ range. The square root of the rate derivative $\Psi^{0.5}$ and the wave speed v depend on θ in a qualitatively similar fashion. At fixed θ, $\Psi^{0.5}$ is larger for higher values of h_0 and for lower values of A_0. This behavior can be explained by the dissociation of $HBrO_3$ and its effect on the term k_5h_0AX, which corresponds to autocatalytic production of X. This term increases more with increasing h_0 than with increasing A_0.

Figure 6 shows that in the ferroin-catalyzed BZ reaction the wave speed passes through a maximum as θ increases, while $\Psi^{0.5}$ remains proportional to $\theta^{0.5}$.

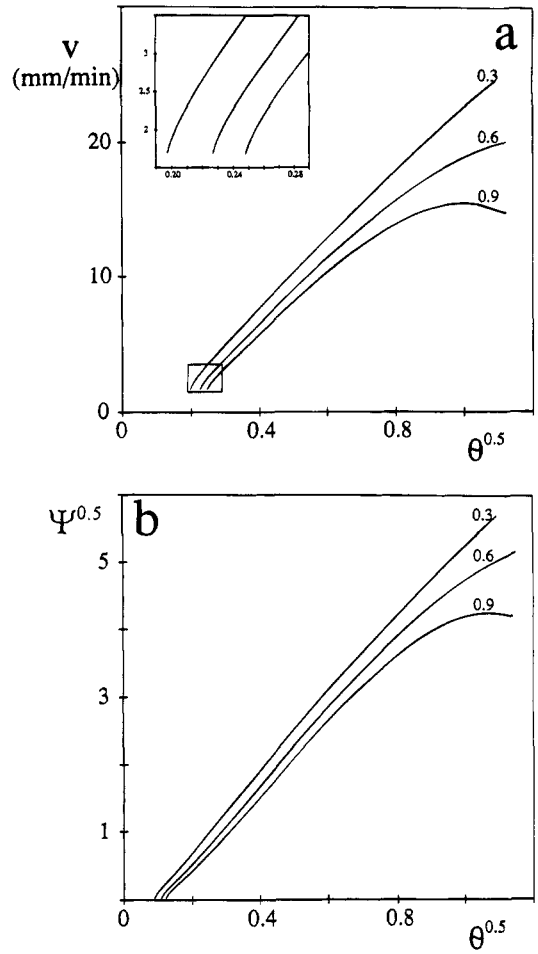

Figure 3. Dependence of the wave speed v (a) and the square root of the rate derivative $\Psi^{0.5}$ (b) on $\theta^{0.5} = (h_0A_0)^{0.5}$ for fixed A_0 in the Ce-catalyzed BZ reaction; $C = 6 \times 10^{-3}$ M, $q = 1.2$; values of A_0 (M) are shown in the figure.

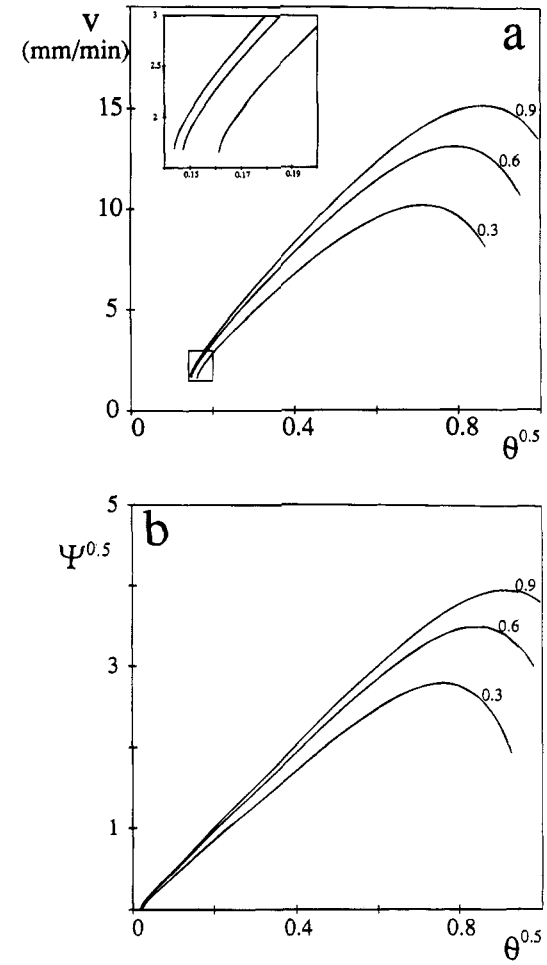

Figure 4. Dependence of v (a) and $\Psi^{0.5}$ (b) on $\theta^{0.5}$ for fixed h_0 in the Ce-catalyzed BZ reaction; $C = 6 \times 10^{-3}$ M, $q = 1.2$; values of h_0 (M) are shown in the figure.

Experimental Results

Dependence of SOW Region on Oxygen. Our calculations show that the dependence of wave speed on $\theta^{0.5}$ should deviate from linearity, due to an increase of the excitation threshold. This behavior occurs near the boundaries of the SOW region, where the amplitude of the wave is rather small. To increase the sensitivity of our experiments by enhancing optical contrast, we used a solution layer twice the thickness of that employed by Nagy-Ungvarai *et al.*[6] As a result of this change, our experiments yield a significant decrease of the SOW region compared with the data of ref 6.

It is known that oxygen strongly promotes the production of Br^- in the BZ reaction[19] and that O_2 is consumed during the BZ reaction.[20] Consequently, the effect of the layer thickness enhancement could be a result of the decrease of oxygen concentration near the bottom of the layer.

To check this supposition we determined the boundaries of the SOW region in the (h_0,A_0)-plane in the Ce-catalyzed BZ reaction–diffusion system run with and without oxygen. The upper boundary of the SOW region is defined as the lower boundary of the bulk oscillation region. The lower boundary is determined by the ability of a silver wire to initiate a self-sustained wave in the solution. Figure 7a shows the boundaries of the SOW region in a BZ solution layer exposed to air. Figure 7b shows that the SOW region is much narrower in the same BZ solution layer placed between two glass plates. The concentration of H_2SO_4 used in the experiments was transformed to a Hammett acidity function h_0.

Fitting Boundaries of the Experimental Region of SOW. As noted in the Simulation Results section, we assume that the upper boundary of the SOW region coincides with the calculated Hopf line, and a calculation of this boundary is shown for the h_0,A_0-plane (Figure 1a). The lower calculated boundary was found by direct simulation of wave propagation. The positions of these calculated boundaries depend on the stoichiometric factor q. Figure 7a,b shows the experimentally determined behavior (oscillation, SOW, or no spatial effects) and the calculated boundaries of the SOW region. The fitting gives $q = 1.0$ for the layer exposed to air, and $q = 0.6$ for the layer placed between glass plates. This experimental result corresponds very well with the assumed effect of oxygen on the stoichiometric factor.

Discussion

There are a number of papers dealing with the BZ wave speed dependence on the combined variables A_0 and h_0.[1-6] However, only those of Field and Noyes[1] and Nagy-Ungvarai *et al.*[6] utilize a wide enough range of concentrations to evaluate the dependence. Field and Noyes[1] present the following best fit of their data: $v = -0.832 + 27.87\theta^{0.5}$ (in mm/min). Figure 5a shows that in their concentration range our model gives virtually linear dependence. The linear fit of our numerical data yields the following comparisons: $v = -0.983 + 20.78\theta^{0.5}$ for variable A_0 and $h_0 = 0.365$ M, and $v = -3.030 + 27.92\theta^{0.5}$ for variable h_0 and $A_0 = 0.3$ M. The results show rather good quantitative coincidence.

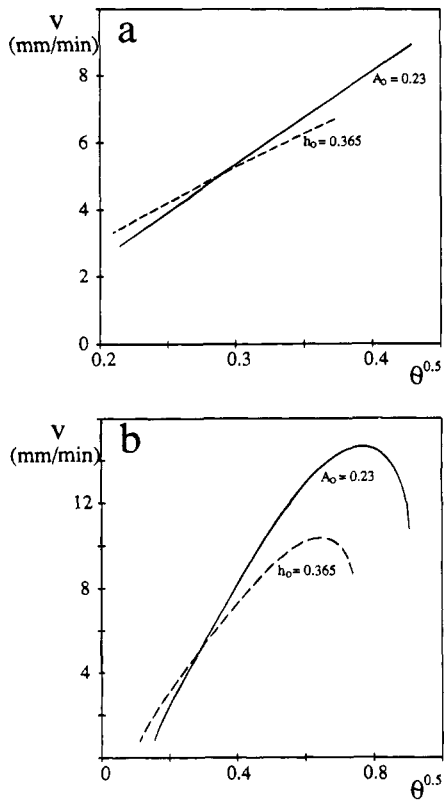

Figure 5. Calculated dependence of v on $\theta^{0.5}$ in the ferroin-catalyzed BZ reaction–diffusion system; $C = 2 \times 10^{-3}$ M, $q = 1.2$. Dashed line, $h_0 = 0.365$ M; solid line, $A_0 = 0.23$ M. (a) Field–Noyes experimental range;[1] (b) entire range of excitability.

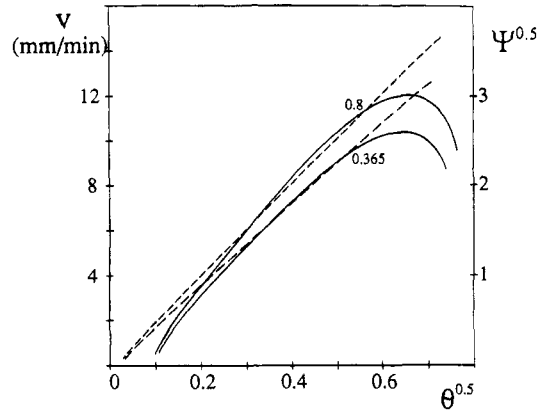

Figure 6. Dependence of v (solid lines) and $\Psi^{0.5}$ (dashed lines) on $\theta^{0.5}$ for $h_0 = 0.365$ M and $h_0 = 0.8$ M in the ferroin-catalyzed BZ reaction; $C = 2 \times 10^{-3}$ M, $q = 1.2$.

In the experiments of Nagy-Ungvarai *et al.*[6] in the range $\theta^{0.5} = 0.18-0.52$ the wave velocity above 0.38 increases more slowly with increase in concentration variables than in the lower portion of the range. In the range 0.18–0.38, the experimental data can be best fit by the equation $v = -2.1 + 22.5\theta^{0.5}$. The linear fit of the corresponding simulation in the range 0.2–0.38 is $v = -3.4 + 27.85\theta^{0.5}$.

Therefore, in the range where the linear approximation is valid, the results of our simulations are in good agreement with the experimental data.

The simulations show deviations from linearity at both ends of the range of the pulse propagation. The lower values of A_0 and h_0 correspond to high values of the excitation threshold and low wave speed. Figures 3 and 4 show a slight deviation from linearity near the boundary of propagation. Experimentally, this effect should prove difficult to confirm, because it is

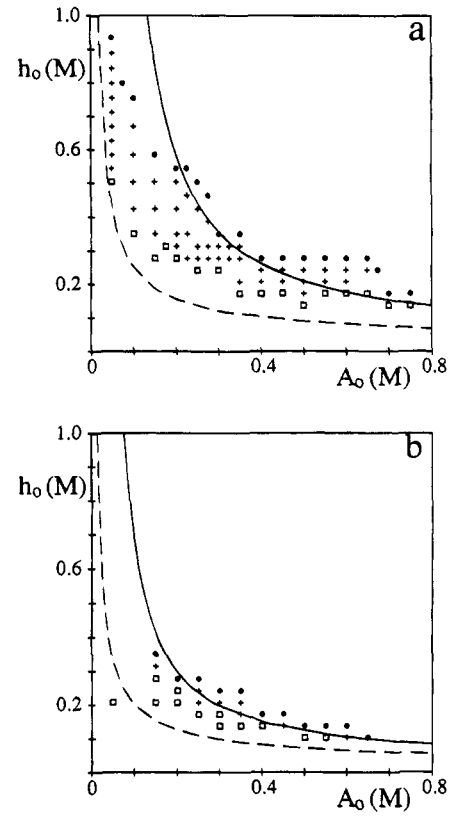

Figure 7. Regions of self-sustained propagation of solitary oxidation waves (SOW) in the Ce-catalyzed BZ reaction–diffusion system. Experiment: circles, bulk oscillations; crosses, SOW; squares, no waves were detected; (a) reactive layer open to air, (b) same layer between glass plates. Simulations: solid line, Hopf bifurcation; dashed line, lower boundary of the SOW region; (a) $q = 1.0$, (b) $q = 0.6$.

small and confined to a narrow range of initial reagent concentrations.

At high values of A_0 and h_0 the simulations show a significant deviation from linearity leading to a maximum in the velocity. Experimentally, this region is more accessible, although until now such measurements were not done because they are limited by the emergence of bulk oscillations at high θ[1,4,5]. Our data, together with those of ref 6, show that it is possible to extend the region of SOW at high θ by increasing the oxygen concentration in the reactive layer. Our simulations suggest that it should be possible to eliminate the oscillatory region, preserving a large region of SOW. Another limitation is the very high concentration of bromate necessary to reach the maximum of the wave speed at relatively low values of acidity that have so far been employed in studies of ferroin waves. Figure 6 shows that a curve with a maximum should be obtainable with $h_0 \geq 0.8$ M at reasonable concentrations of bromate.

In the model of the ferroin-catalyzed BZ system, the maximum in speed appears while the first derivative of the rate of autocatalysis (Ψ) remains proportional to $\theta^{0.5}$ (Figure 6). The significance of this finding is that appearance of the maximum is due to increase of the ratio of the excitation threshold to the amplitude of the pulse. Diminution of the pulse width can also be partly responsible for the effect. Therefore, for the ferroin-catalyzed BZ reaction, our model of chemical wave propagation (Figure 2) predicts a wave speed concentration dependence significantly different from that of the rate of the leading autocatalytic reaction. In the cerium-catalyzed BZ system, however, the dependencies of v and of the square root on the first derivative of the autocatalysis rate (Ψ) qualitatively

coincide. For this system, therefore, it is difficult to separate any effects of the excitation threshold and the pulse width.

Conclusion

We have analyzed for the first time the pulse speed dependence on concentration in the full range of concentrations. In the concentration ranges of the previous experimental measurements the numerically determined dependence is practically linear and in good agreement with experimental data. We found deviations from a linear dependence of the speed on the square root of the product of acidity and total bromate concentration $\theta = (h_0[BrO_3^-]_T)^{0.5}$ both for high and low θ. A maximum of the wave speed is predicted both for cerium- and ferroin-catalyzed BZ reaction diffusion systems. To check the prediction, the experiments must be done with reaction mixtures saturated by oxygen to significantly increase the region where solitary oxidation waves propagate.

Acknowledgment. This work was supported by the National Science Foundation through research (CHE-9304087 and CHE-9023294) and U.S.−Czechoslovakia cooperative (INT-8912462) grants, and by a summer fellowship (M.S.) from the National Institutes of Health (2S03RR03373-10).

References and Notes

(1) Field, R. J.; Noyes, R. M. *J. Am. Chem. Soc.* **1974**, *96*, 2001.
(2) Ortoleva, P.; Schmidt, S. In *Oscillations and Traveling Waves in Chemical Systems*; Field, R. J., Burger, M., Eds.; Wiley: New York, 1985; p 333.
(3) Kuhnert, L.; Krug, H. J. *J. Chem. Phys.* **1987**, *91*, 730.
(4) Ševčikova, H.: Marek, M. *Physica D* **1983**, *9*, 140.
(5) Wood, P. M.; Ross, J. *J. Chem. Phys.* **1985**, *82*, 1924.
(6) Nagy-Ungvarai, Z.; Tyson, J. J.; Hess, B. *J. Phys. Chem.* **1989**, *93*, 707.
(7) (a) Fisher, R. A. *Ann. Eugenics* **1937**, *7*, 355. (b) Kolmogorov, A. N.; Petrovsky, I. G.; Piskunov, N. S. *Bull. Moscow State Univ.; Mat. Mech.* **1937**, *1*, 1.
(8) Frank-Kamenetsky, D. A. *Diffusion and Heat Transfer in Chemical Kinetics*; Science Publ.: Moscow, 1967.
(9) Saul, A.; Showalter, K. In *Oscillations and Traveling Waves in Chemical Systems*; Field, R. J., Burger, M., Eds.; Wiley: New York, 1985; p 419.
(10) Gray, P.; Scott, S. K. *Chemical Oscillations and Instabilities*; Oxford University Press: Oxford, England, 1990.
(11) Tyson, J. J. In *Oscillations and Traveling Waves in Chemical Systems*; Field, R. J., Burger, M., Eds.; Wiley: New York, 1985; p 93.
(12) Försterling, H.-D.; Stuk, L.; Barr, A.; McCormick, D. *J. Phys. Chem.* **1993**, *97*, 2623.
(13) Zhabotinsky, A. M.; Buchholtz, F.; Kiyatkin, A. B.; Epstein, I. R. *J. Phys. Chem.* **1993**, *97*, 7578.
(14) Robertson, E. B.; Dunford, H. B. *J. Am. Chem. Soc.* **1964**, *86*, 5080.
(15) Tyson, J. J.; Keener, J. P. *Physica D* **1988**, *32*, 327.
(16) Marek, M.; Schreiber, I. *Chaotic Behavior of Deterministic Dissipative Systems*; Cambridge University: Cambridge, U.K., 1991.
(17) Hindmarsh, A. C. In *Scientific Computing*; Stepleman, R. S., et al., Eds.; North-Holland: Amsterdam, 1983; p 55.
(18) Zhabotinsky, A. M.; Györgyi, L.; Dolnik, M.; Epstein, I. R. *J. Phys. Chem.* **1994**, *98*, 7981.
(19) Ganapathisubramanian, N.; Noyes, R. M. *J. Phys. Chem.* **1982**, *86*, 5158.
(20) Kuhnert, L.; Pohlmann, L.; Krug, H.-J. *Physica D* **1988**, *29*, 416.